J Nanopart Res (2012) 14:989
DOI 10.1007/s11051-012-0989-z

RESEARCH PAPER

Exposure assessment and engineering control strategies for airborne nanoparticles: an application to emissions from nanocomposite compounding processes

Candace S.-J. Tsai · David White · Henoc Rodriguez · Christian E. Munoz · Cheng-Yu Huang · Chuen-Jinn Tsai · Carol Barry · Michael J. Ellenbecker

Received: 6 December 2011 / Accepted: 11 June 2012 / Published online: 1 July 2012

Abstract In this study, nanoalumina and nanoclay particles were compounded separately with ethylene vinyl acetate (EVA) polymer to produce nanocomposites using a twin-screw extruder to investigate exposure and effective controls. Nanoparticle exposures from compounding processes were elevated under some circumstances and were affected by many factors including inadequate ventilation, surrounding air flow, feeder type, feeding method, and nanoparticle type. Engineering controls such as improved ventilation and enclosure of releasing sources were applied to the process equipment to evaluate the effectiveness of control. The nanoparticle loading device was modified by installing a ventilated enclosure surrounding the loading chamber. Exposures were studied using designed controls for comparison which include three scenarios: (1) no isolation; (2) enclosed sources; and (3) enclosed sources and improved ventilation. Particle number concentrations for diameters from 5 to 20,000 nm measured by the Fast Mobility Particle Sizer and aerodynamic particle sizer were studied. Aerosol particles were sampled on transmission electron microscope grids to characterize particle composition and morphology. Measurements and samples were taken at the near- and far-field areas relative to releasing sources. Airborne particle concentrations were reduced significantly when using the feeder enclosure, and the concentrations were below the baseline when two sources were enclosed, and the ventilation was improved when using either nanoalumina or nanoclay as fillers.

Keywords Airborne nanoparticle · Nanoalumina · Nanoclay · Nanocomposite compounding · Inhalation exposure · Engineering control

Electronic supplementary material The online version of this article (doi:10.1007/s11051-012-0989-z) contains supplementary material, which is available to authorized users.

C. S.-J. Tsai (✉) · M. J. Ellenbecker
NSF Center for High-rate Nanomanufacturing (CHN), University of Massachusetts Lowell, One University Avenue, Lowell, MA 01854, USA
e-mail: candace.umass@gmail.com

D. White · C. Barry
Department of Plastics Engineering, University of Massachusetts Lowell, Lowell, MA, USA

H. Rodriguez · C. E. Munoz
Industrial Microbiology Department, University of Puerto Rico Mayagüez, Mayagüez, Puerto Rico

C.-Y. Huang · C.-J. Tsai
Institute of Environmental Engineering, National Chiao Tung University, Hsinchu, Taiwan

Introduction

A nanocomposite is defined as a composite material in which the reinforcing agents are nanoparticles. Nanocomposites have the potential to be implemented as new high-strength replacements for traditional

composites. One of the most important aspects of creating a functional nanocomposite is to disperse the reinforcing agent throughout the entire bulk of the polymer during processing, so each particle is wetted completely by the liquid polymer. If clusters are avoided then the small diameter of the particles themselves will contribute a very high-interfacial surface area and, in theory, improve the mechanical properties of the polymer (McCarrie and Winter 2003).

The ongoing nanocomposite research performed at the University of Massachusetts Lowell associated with the Center for High-rate nanomanufacturing typically involves a large quantity of nanoparticles being dispersed into polymers. During previous experiments in our laboratories, exposures from compounding processes were elevated under some circumstances and were affected by many factors including inadequate ventilation, surrounding air flow, feeder type, feeding method, and nanoparticle type (Tsai et al. 2008a, b). The work reported here was performed in a new pilot plant facility launched in 2009.

During these experiments, airborne particles associated with the reinforcing nanoparticles in addition to polymer fumes are of particular concern, as they can readily enter the body through inhalation. A very small size makes it easier for the particles to penetrate into the interstitium, and the small particles can evoke higher inflammation and overall toxicity (Ferin et al. 1990). Much greater inflammation and cardiopulmonary health effects have also been observed for metal nanoparticles compared to larger respirable particles (Ferin et al. 1991; Zhang et al. 2000; Wolff et al. 1988). Particle deposition modeling indicates that up to 90 % or more of the inhaled mass fraction of particles smaller than 100 nm will deposit in the human respiratory tract, with up to approximately 50 % in the alveolar region (ICRP 1994). Particles of about 20–30 nm in diameter deposit more readily in the alveoli than particles of ca. 200–500 nm. Small particles usually form agglomerates, and their agglomerated size determines their airway deposition. If the primary particle size is ca. 20–30 nm, deagglomeration may affect the translocation of the particles more than for intact agglomerates consisting of larger particles (Ferin et al. 1990). A report by Takenaka et al. (1986) indicated that such agglomerates of ultrafine-inhaled insoluble particles can deagglomerate in the lung and the primary particles can be found to a significant degree in the interstitium. Oberdorster et al. (1990) and Renwick et al. (2004) also concluded that dusts consisting of ultrafine particles (nanoalumina) induce a more severe adverse pulmonary effect than larger sized particles of the same dusts. The particle size can be a decisive parameter for the induction of adverse pulmonary effects, even by so-called "nuisance" dusts. Takenaka et al. (1986) recommends that occupational exposure standards for "nuisance" dusts should be reconsidered to take into account the possibly damaging effects of ultrafine particles.

Engineering controls are essential to limit releases from compounding processes. Maynard and Kuempel (2005) concluded that aerosol control methods have not been well characterized for nanometer-sized particles, although theory and limited experimental data indicate that conventional ventilation, engineering control, and filtration approaches should be applicable in many situations. During twin-screw extrusion of nanocompounds, the environmental emissions of airborne nanoparticles and high-operator exposures were found to include primary airborne nanoparticles, clusters of nanoparticles, and polymer fume (Tsai et al. 2008a), and such exposures were affected by the feeding method (Tsai et al. 2008b). Our previous work (Tsai et al. 2008b) showed that applying a pilot containment method to the extruder feeder could reduce the concentration of released nanoparticles by four orders of magnitude. Well-designed enclosures and improved ventilation were employed in the current study, where two types of nanoparticles, i.e., nanoalumina and nanoclay, were compounded with a polymer using a twin-screw extruder (TSE). Nanoclay, which disperses into the polymer as nanometer-thin sheets with areal dimensions of 2–13 μm, was used for comparison with the spherical nanoalumina (nano-aluminum oxide) particles.

For a process such as the compounding extruder, workers' exposure to toxic substances released from a certain source will be affected by the airflow patterns surrounding the workers. The exposure extending between the releasing source and the worker's breathing zone (BZ), called the "near-field," has been studied for various toxic substances (Bottini et al. 2003). The dilution of contaminants in this near-field vicinity depends upon several factors. The most obvious factors are the workers' proximity to the

source and their orientation with respect to its plume (upwind or downwind) and the magnitude of air turbulence (Popendorf 2006). Kim and Flynn (1991a, b) found that eddies in the wake of obstacles such as people extend perhaps two body widths downwind.

During the compounding operation, operators were moving around the immediate vicinity of the machine; thus, the near-field vicinity was defined as the radius of the area where operators could position themselves naturally to load materials and operate the machine, which was less than 0.5 m from the source edge. The evaluation of the effectiveness of using engineering controls was performed by measuring nanoparticle concentrations at locations in the near-field area and locations away from the source, called the far-field area.

Materials and methods

Materials and equipment

Model nanocomposite systems consisting of ethylene vinyl acetate (EVA) (ELVAX 450, Dupont) and nanoalumina or nanoclay were employed in this study. The nanoalumina (Al_2O_3), obtained from Nanophase Technologies Corporation (grade Al-015-003-025), was manufactured using physical vapor synthesis (PVS). The nanoalumina particles were roughly spherical in shape with an average primary particle size ranging from 27 to 56 nm.[1] The typical size of agglomerates was measured to be around 200 nm. The nanoclay (Cloisite 20A), obtained from Southern Clay Product Inc (www.nanoclay.com), was a natural montmorillonite modified with a quaternary ammonium salt. Each experiment used about 200–300 g of EVA mixed with 5 % by weight of nanoparticle.

Standard industrial equipment including a 30-mm co-rotating TSE (Werner & Pfleiderer, Model: ZSK-30) with a strand die, a twin-screw volumetric feeder, a water bath, and a belt puller was used to compound polymer nanocomposites. During the twin-screw extrusion process, the polymer pellets and nanoparticles were premixed in a fume hood and fed under gravity from the feeder into the feeding funnel of the extruder. In the original configuration, this feed path was open to the environment. The mixed melt was then forced through the die, forming a strand. This strand was then cooled and solidified as it was pulled through the water bath by the belt puller. Strand pelletizing equipment, which is typically attached to the line, was not used during the monitored experiments (the strands were pelletized in a separate step). The TSE consists of two co-rotating screws in a metal barrel which contains heating elements and water cooling. This extruder has two feed or vent ports. The polymer and filler mixture were melted by shearing elements in the first sections of the screws. Due to the incorporation of reverse pitched conveying elements in the screw program, however, most of the air fed into the extruder during feeding must be vented back through the second feed port.

Engineering controls studied

Several different engineering controls were studied in order to compare exposures to the original configuration where limited controls were used. For the original configuration, the first scenario, called the *no-isolation* scenario, the nanoparticles and polymer mixture for compounding process, were manually loaded into the feeder from the top and fed into the extruder through the throat falling into the open funnel (Fig. 1a, arrow). Ventilation control was supplied by a flexible duct attached to the existing room overhead exhaust system and placed as close as possible to the hopper and feeder, as shown in Fig. 1a. This venting system provided exhaust air flow of 11.3 m^3/min (400 ft^3/min) through the 15-cm (6 in.) ventilation duct and was running for all experiments (except one trial for nanoclay) to provide the same air exchange rate in the room.

The second scenario, using control called the *feeder enclosure*, is shown in Fig. 1b. The custom made enclosure, design shown in Fig. 2, was made using a plastic bottle attached with a large elastic rubber balloon (cut at top and bottom) to tightly enclose the feeding throat and the funnel top opening.

The third scenario, using control called the *full enclosure*, was to enclose the material loading to the open-top twin-screw feeder in addition to the *feeder enclosure*. The manual loading of the mixed polymer and nanoparticles to the feeder was replaced using an enclosed hopper containing the mixed materials placed on the top of the feeder to load materials into

[1] Nanophase company website: www.nanophase.com/technology/capabilities.asp.

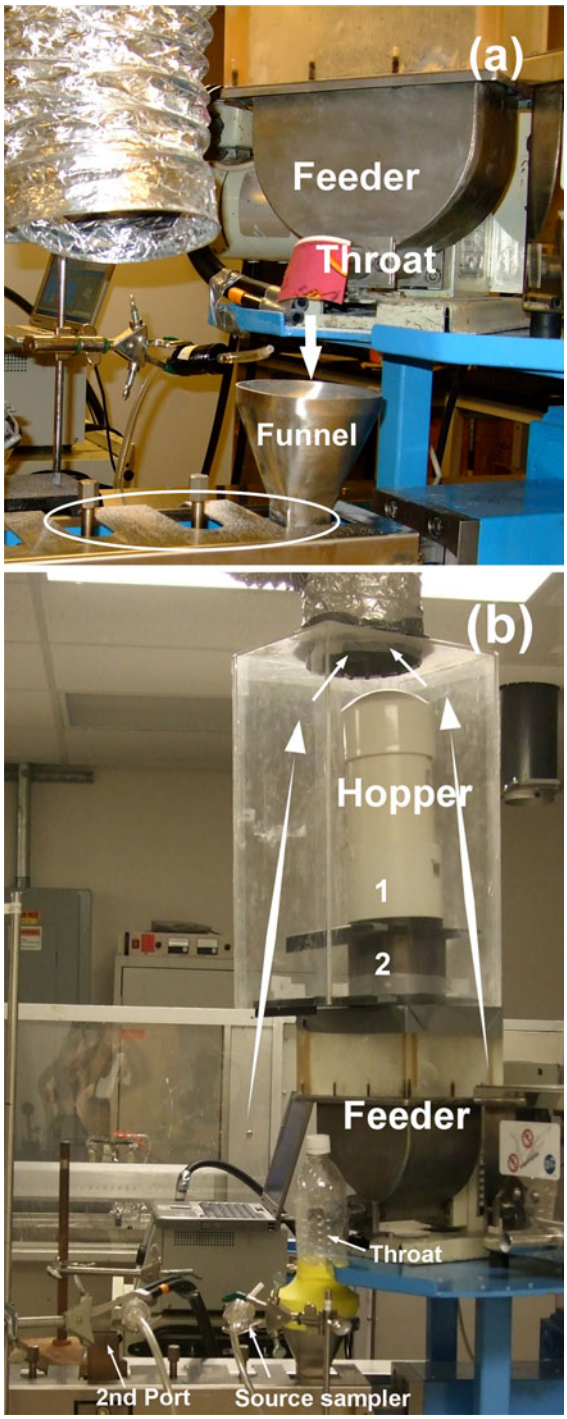

Fig. 1 Set-up of equipment. **a** Feeder set-up with *no isolation*; **b** feeder and hopper set-up with enclosures and ventilation for *feeder enclosure* and *full enclosure* tests, and locations of source sampler and the 2nd port

the feeder, as shown in Fig. 1b. The design of the enclosed hopper is shown in Fig. 2. The hopper was built to include two compartments labeled 1 and 2 in Fig. 1b; materials were mixed and placed in the top compartment inside a constant velocity fume hood, enclosed by a blast gate, then the bottom compartment was attached and enclosed using a second blast gate. Materials were loaded in two steps, from the first to the second compartment, and then were fed into the feeder by opening the two blast gates in sequence. The acrylic enclosure was placed over the hopper and sat on the feeder top which gave two open side slots, each with dimensions of 3.8 cm × 20 cm. A ventilation duct was connected to the top of the acrylic enclosure allowing air to flow over the feeder into the acrylic enclosure as shown by the arrows in Fig. 1b. The vented air flow through the hopper enclosure was the same maximum available from the overhead exhaust system, i.e., 11.3 m^3/min (400 ft^3/min) and it provided a velocity of 750 m/min (2460 ft/min) through the open slots. The *full enclosure* control was ventilated for two nanoalumina compounding trials, but the ventilation was turned off during one nanoclay compounding trial to compare the effectiveness of the enclosure without ventilation.

Analysis of capture velocity

In addition to ensuring that any particle release inside the enclosure is controlled, the exhaust ventilation entering the two slots can capture airborne particles released elsewhere in the system, such as at the second feed port which was used for pressure release during these experiments. The capture velocity as a function of distance from a slot hood can be calculated using the Silverman equation (Burgess et al. 2004):

$$V(x) = \frac{Q}{3.7Lx} \quad (1)$$

where x is the distance from the slot hood to the source (m), $V(x)$ capture velocity at distance x (m/min), Q air flow (m^3/min), and L length of the slot (m).

Particle measurement and data analysis

The concentrations of airborne nanoparticles were measured every second by two instruments, i.e., the

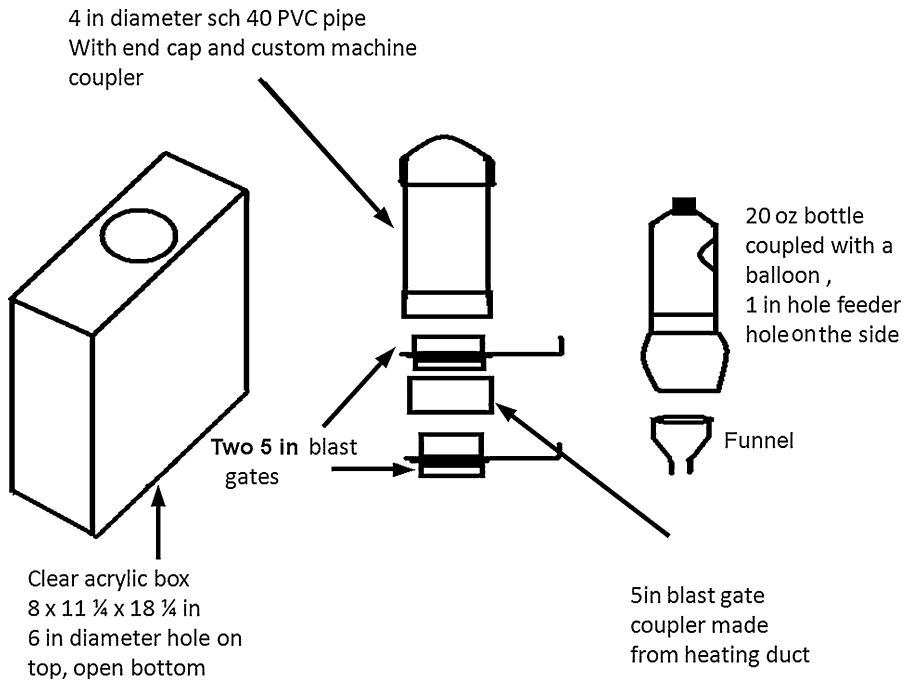

Fig. 2 Illustration of design of feeder and hopper enclosures for feeding and loading materials

Fast Mobility Particle Sizer (FMPS™) spectrometer (Model 3091, TSI) and the Aerodynamic Particle Sizer (APS®) spectrometer (Model 3321, TSI), simultaneously to obtain data for particle diameters from 5.6 nm to 20 μm. The APS provides high-resolution, real-time aerodynamic measurements of particle size. The FMPS performs particle size classification based on differential electrical mobility classification. Measurements were taken after the warm-up of the TSE, during loading materials and during nanocomposite compounding at various locations in the near- and far-field areas as shown in Fig. 3. Two pieces of 3-m long Tygon® tubing were connected to the air inlets of the FMPS and APS to reach the measurement locations. Our investigation about particle loss in this tubing was found to be minimal for particles larger than 20 nm, and only relative data were used for comparison in this study to avoid the effect of particle loss. Normalized particle number concentrations were calculated and averaged in each of the 32 size channels for each 2 min (120 data points) measurement, and each measurement was repeated at the same location. The concentrations measured at each location during the time period after extruder warm-up and before loading materials to the extruder were used as the "baseline" of each location for subtraction from subsequent concentration measurements. The baseline total concentration data are listed in Table 1, baseline column. The exposure concentrations were measured before and after applying engineering controls to compare the performance, i.e., no isolation, using the feeder enclosure and using the full enclosure (feeder and hopper). Measurements were taken at various locations, i.e., hopper source and feeder source for near-field, and far-field includes the 2nd port, BZ, and room background (BG). BZ and source locations were at 130 cm and 124 cm height above the floor (Fig. 3), respectively. The measurements taken at sources represent the highest near-field exposure. The measurements taken at the BZ represent the highest far-field exposure since the dilution was extended downwind from the BZ. Correlations among concentration data obtained from various locations and using various control methods were statistically analyzed using the Pearson correlation coefficient (γ).

Particle characterization and sample analysis

Nanoparticle aerosol filter samplers were used to collect airborne nanoparticles (Tsai et al. 2009). Transmission electron microscope (TEM) copper grids (SPI 400 mesh with a formvar/carbon film) were

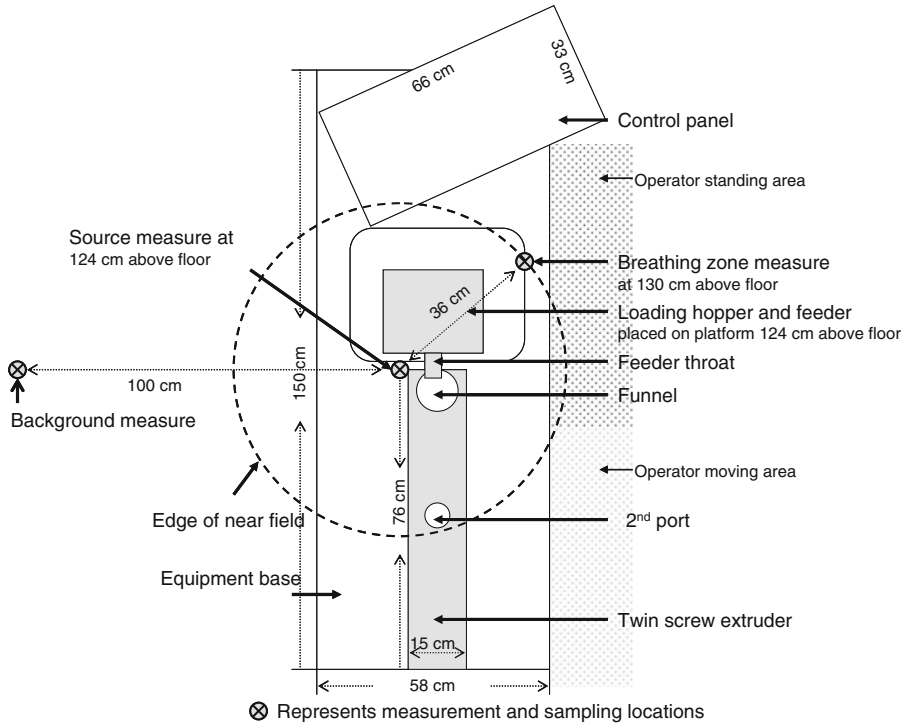

Fig. 3 Illustration of near- and far-field measurement locations and equipment layout

taped on 47 mm diameter polycarbonate membrane filters (0.2 μm pore size) and attached with fiber backing filters. Air flow was driven by a pump at a flow rate of 0.3 L/min, and particles were collected on the grid for analysis. Sampled particles were characterized using TEM and energy dispersive spectroscopy (EDS). TEM images of the samples were taken using a Philips EM400 TEM (Eindhoven, The Netherlands) operated at 100 kV. For EDS analysis of particles attached to the TEM grids, a Thermo-Noran EDS system (Waltham, MA) having a 40-mm^2 SiLi detector and a Noran System Six X-ray Spectral Acquisition System V2 was used to acquire EDS spectra from particles excited by a nano-sized ($\sim$10 nm) electron beam probe of the TEM.

Results and discussion

Exposure affected by engineering controls

Three releasing sources were identified, i.e., the feeding throat, the feeder open top for loading, and the second feeding port for gas venting. Near- and far-field exposure concentrations with various engineering control methods were compared to no isolation at those releasing sources to evaluate the effectiveness of those methods. Qualitatively, it was observed that the surface of the extruder top around the funnel area was con taminated with white nanoalumina particles released from the feeding procedure without using isolations as seen in the circle marked in Fig. 1a. Total particle number concentration changes measured by the FMPS and APS at various locations were adjusted by subtracting the baseline concentration of each location (concentration after warming up the extruder and before loading materials) to give the adjusted total concentration, and the resulting data are shown in Table 1, the "change" column, where a negative number indicates that measured concentrations were below the baseline concentrations. Each experiment was performed on a different day; as noted in the table, the baseline concentration varied considerably from day to day. Small negative numbers, such as those found here, are due to the inherent variability in the baseline concentration within 1 day and indicate that the measured particle release was essentially zero. Total particle concentrations were reduced significantly at all locations

Table 1 Total particle number concentrations (particle diameters from 5 to 560 nm) affected by engineering controls: comparison of near- and far-field measurements for nanoalumina and nanoclay compounding

	Total particle number concentration (particles/cm^3)							
	No isolation		Feeder enclosure		Full enclosure 1st trial		Full enclosure 2nd trial	
	Baseline	Change	Baseline	Change	Baseline	Change	Baseline	Change
(a) Nanoalumina								
Loading near-field								
Hopper source	8,330	17,280	2,600	8,590	250	−810	1,080	−40
Loading far-field								
BZ	7,780	980	3,490	1,070	350	−910	1,330	−460
Processing near-field								
Feeder source[a]	7,210	6,060	4,410	360	430	−520	1,480	−340
Processing far-field								
BG[a]	7,780	2,160	3,490	−1,140	350	−740	1,330	−410
BZ[a]	8,330	1,080	2,600	−540	250	−502	1,080	−490
2nd port[a]	8,560	1,070	3,780	−710	350	−490	1,350	−590
(b) Nanoclay								
Loading near-field								
Hopper source	2,010	130,980	590	3,320	260[b]	100[b]	2,850	−300
Loading far-field								
BZ	2,180	12,390	760	−150	390[b]	−40[b]	2,800	−200
Processing near-field								
Feeder source[a]	1,550	97,380	860	−20	420[b]	0[b]	3,230	−340
Processing far-field								
BG[a]	2,180	26,190	760	−140	390[b]	20[b]	2,800	−490
BZ[a]	2,010	16,130	590	−120	260[b]	−50[b]	2,850	−180
2nd port[a]	1,840	16,090	750	2,580	350[b]	30[b]	2,980	−280

All data were adjusted by subtracting the before-process baseline data

[a] Data sets were analyzed using Pearson correlation

[b] Ventilation was turned off for this trial

when feeder enclosure was applied (Table 1). Since enclosing the feeder eliminated the immediate escape through the feeder mouth during loading, concentration reduction was observed to be significant for the loading procedure. For processing, the concentration change at feeder source was reduced from 6,060 to 360 particle/cm^3 during processing nanoalumina compounding and from 97,380 to −20 particle/cm^3 during nanoclay compounding (Table 1, no isolation and feeder enclosure columns). More concentration reductions were seen when full enclosures were applied for both nanoalumina and nanoclay compounding.

When using the full enclosure, the total concentrations were below or just slightly above the baseline as shown in Table 1. The ventilation was used for the full enclosure tests except for one trial of nanoclay compounding as noted in Table 1. For nanoalumina compounding, the total concentration changes during the full enclosure tests were several hundred particles below the baseline and were more than three orders of magnitude below the no-isolation test and in a comparable range for the two repetitions (Table 1a). For nanoclay compounding, the unventilated full enclosure reduced concentrations close to the baseline, while the ventilated full enclosure reduced concentrations more than three orders of magnitude below the no-isolation test (Table 1b).

Correlations of the concentration profiles (5–560 nm) of released particles from tests using various control methods and at various locations were analyzed using Pearson correlation. Correlations evaluated in the

analyzed data set are noted with single subscript star symbol linked to the location names in Table 1; the complete results of the statistical analysis are available in the Supplementary Information (SI). The results show that particle concentration profiles of various scenarios (no isolation, feeder enclosure, and two full enclosure trials) taken at the same location (i.e., feeder source) did not have strong correlations which indicates that the released-particle profiles were independent of each other when various control methods were applied. Such results were found consistently for all individual locations and both nanoalumina and nanoclay compounding, where none of Pearson coefficients (γ) are above 0.9 (SI).

However, when comparing the concentration profiles of four locations (feeder source, BG, BZ, and 2nd port) when measured under the same control method (i.e., feeder enclosure and full enclosure), strong correlations were found with Pearson coefficients above 0.9. In the case of nanoalumina compounding, the concentration profiles of the no-isolation test showed very low correlations among four locations which likely is due to the particle concentration gradient and agglomerates when moving from the source to the BZ and the 2nd port. When those profiles became strongly correlated ($\gamma > 0.9$), i.e., for the tests using the feeder enclosure and the two full enclosure trials, this indicates that the control methods substantially reduced the particle releases to a comparable magnitude at these four locations for nanoalumina compounding.

In the case of nanoclay compounding, each condition showed a different outcome; it was surprising to see that the profiles showed high correlations ($\gamma > 0.9$) of the four locations for the no-isolation test which indicates that similar aerosol migration patterns were present in these locations. For the feeder enclosure condition, the profile of the 2nd port was not correlated to other locations, while the BZ and BG profiles had high correlations ($\gamma > 0.9$). When the full enclosure was applied without running the ventilation, none of the location profiles were correlated to each other, but when the ventilation was running for the full enclosure, the BG profile was highly correlated with the feeder source, and the BZ profile was highly correlated with the 2nd port.

Aerosols released from nanoalumina compounding

The particle concentration increases associated with nanoalumina compounding are shown in Fig. 4, which plots the particle number concentration as a function of particle size from 5 nm to 20 μm. Particle concentration at the near-field (source) and at the far-field including the BZ, the BG, and the 2nd port locations is shown in Fig. 4a–d, respectively. The near-field source location measurements were taken at a location about 10 cm from the feeding throat as marked as source sampler in Fig. 1b. The majority of the released particles at the source for the no-isolation test were in the size range of 100–560 nm with a magnitude of 35,000 particles/cm^3 and close to a log-normal distribution. Nanoparticles less than 30 nm in diameter were released at concentrations up to 9,000 particles/cm^3. Such nanoparticle release into the room is of particular concern since their mobility and toxicity are much greater than submicrometer particles, and small nanoparticle agglomerates may deagglomerate in the respiratory tract as discussed above.

Results of this study showed that enclosing the feeder effectively reduced particle release, with particles smaller than 30 nm having less than 500 particles/cm^3 increase over baseline, and particles of 50–500 nm diameter having less than 2,000 particles/cm^3 increase with the mode at 100 nm (Fig. 4a). When the full enclosure was applied, particle increase was barely detected; the particle concentrations were below the baseline for most particle sizes and there was less than a 500-particles/cm^3 increase in nanoparticles smaller than 20 nm at all locations and repeated full enclosure test.

Particles larger than 560 nm diameter had very low concentrations in all measurements. The near-field concentration was one order of magnitude higher than far-field concentrations when tested at no isolation; however, this difference was not seen when the feeder enclosure was applied. In addition, the profile of aerosols for the feeder enclosure condition was shifted with mode at about 100 nm rather than the mode at about 300 nm for no-isolation tests, and the concentrations remained below 2,000 particles/cm^3 for all locations. This indicates that the aerosol releases associated with nanoalumina compounding after applying the feeder enclosure were controlled at a similar magnitude for various locations.

Aerosols released from nanoclay compounding

The concentration of the primary particles released in the near-field (source) from compounding nanoclay composites exceeded 250,000 particles/cm^3 for particle diameters around 100 nm (Fig. 5a) when no

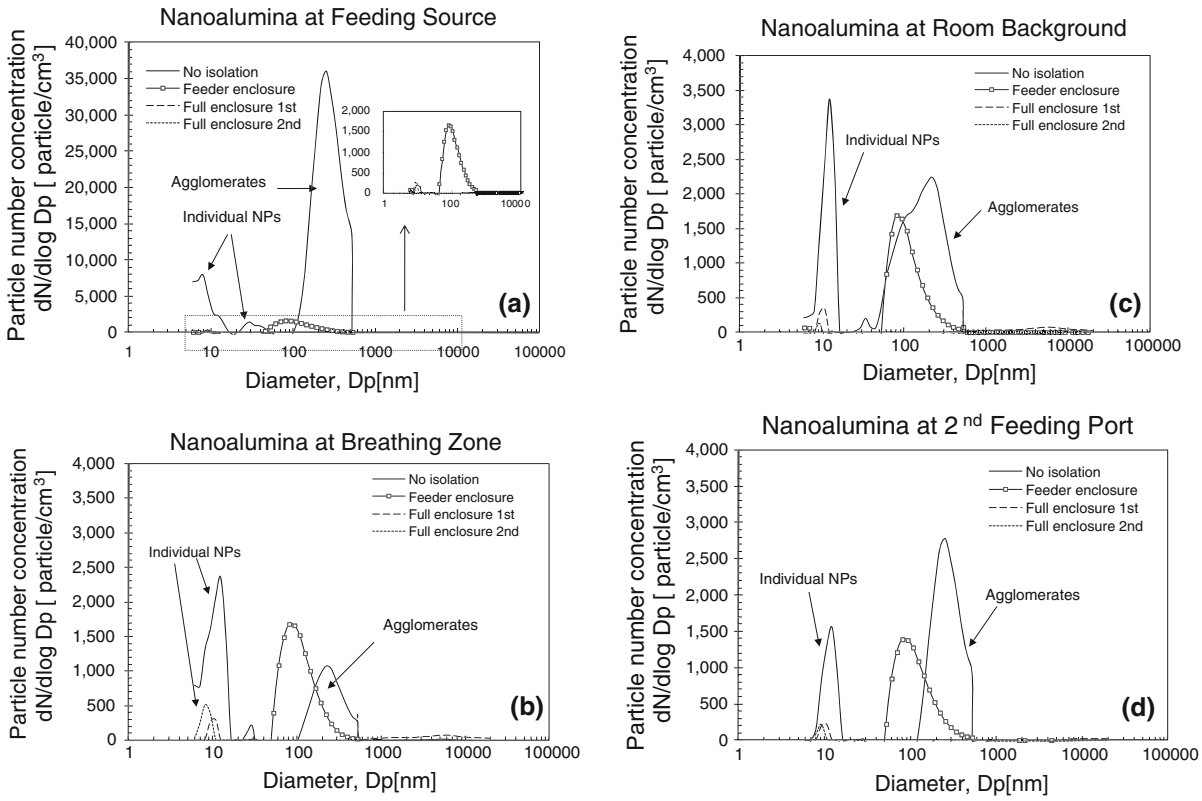

Fig. 4 Particle concentrations and profile associated with *nanoalumina* compounding affected by engineering controls. **a** Near-field at feeding source. **b** Far-field at BZ. **c** Far-field at room BG. **d** Far-field at 2nd feeding port. *NPs* nanoparticles

isolation was used; this is almost a 10-fold increase over the release from compounding nanoalumina. Similar high concentrations were consistently seen in the far-field area (BZ, BG, and 2nd port locations), and the particle concentration profiles showed high correlations with multiple peaks at above 10 nm diameter and around 200 nm diameter as seen in Fig. 5b–d.

Particle release was dramatically reduced to as low as a few hundred particles/cm^3 increase at most near- and far-field locations when the feeder enclosure was applied for nanoclay compounding; however, the peak concentration detected at the far-field, 2nd port, remained high at up to 8,000 particles/cm^3. Releases from nanoclay compounding showed different profiles compared to nanoalumina compounding, while micrometer-sized particles were also barely detected during nanoclay compounding.

Characterization of aerosol particles

Airborne particles collected during nanoalumina and nanoclay compounding were characterized for particle morphology and elemental composition; the results are shown in Figs. 6 and 7, respectively. Airborne nanoalumina particles were found to be released from all trials during nanoalumina compounding, including the tests of *full enclosure* when the particle concentrations were measured to be below the baseline. The TEM images of such collected nanoalumina particles, agglomerates, and individuals are shown in Fig. 6a, b, respectively. Collected airborne particles as shown in Fig. 6c were confirmed to be alumina oxide particles by EDS as seen from the Al signal in Fig. 6d. Individual nanoalumina particles (Fig. 6b) were commonly seen to be released from the 2nd port, which was the venting port releasing high-temperature air and polymer fume. The previous study (Tsai et al. 2008a) performed using an old TSE model in a poorly ventilated laboratory found high quantities of other contaminants such as polymer fumes present in the room aerosols. Typically, polymers would be melted and mixed with well-dispersed nanoparticles when the material being extruded passed the venting port, while

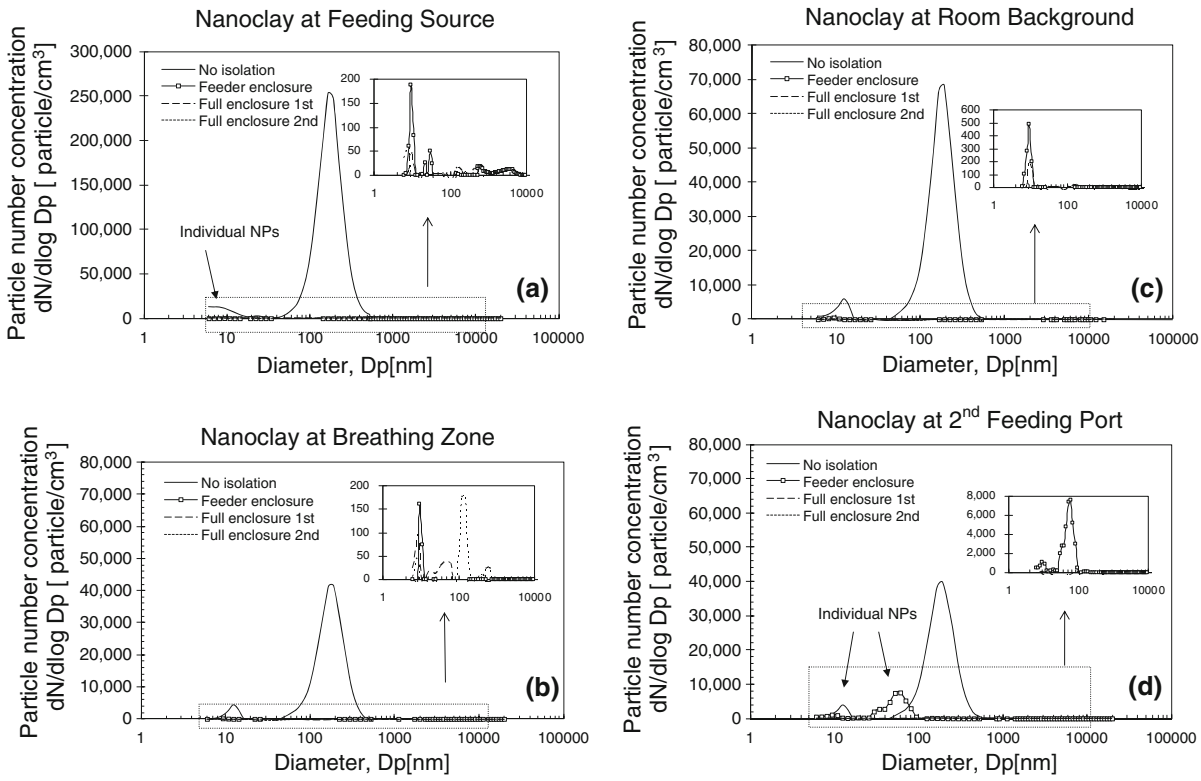

Fig. 5 Particle concentrations and profile associated with *nanoclay* compounding affected by engineering controls. **a** Near-field at feeding source, **b** far-field at BZ, **c** far-field at room BG, and **d** far-field at 2nd feeding port. *NPs* nanoparticles

individual nanoparticles which were not bound with polymer would be released with the heated air and polymer fume into the room through the venting port. The work environment studied here using a new model extruder and a renovated exhaust system in a new laboratory provided a better-controlled environment.

Airborne nanoclay particles were found during the no-isolation and feeder enclosure trials, and were barely found during full enclosure trials. The TEM images of particles collected from the feeder enclosure tests are shown in Fig. 7a, b. Clay particles were dispersed in the polymer in layers of nanometer-thick sheets with areal dimensions greater than a micrometer (2–13 μm according to the manufacturer), but airborne nanoclay particles were smaller than those found in the bulk material. Since the clay particles (Cloisite 20A) contain only 0.1–1 % silica (quartz),[2] the silica EDF response of the few airborne nanoclay particles was barely detectable. The control (bulk) sample of clay particles was generally larger than the small particle shown in Fig. 7c and was characterized by EDS which detected numerous clay particles, and the Si signal can be seen in a low peak in Fig. 7d.

The majority of particles measured during nanoclay compounding were within 100–300 nm diameter (Fig. 5) which was smaller than the size of the airborne nanoclay sheet particles measured in two-dimensional TEM images. This raises the issue of measuring non-spherical aerosols using the FMPS or other similar instruments. Since the FMPS measures particle size through imparting a saturation charge on the particle surface, measuring the resulting electrical mobility and estimating particle size by calculating the diameter of the equivalent spherical particle, such an estimated diameter would be somewhat ambiguous when particles are highly non-spherical. Since relative data are being interpreted in this study, the comparison of particle concentrations under various engineering control methods would not be affected by the shifting of particle diameter by the instrument. However, the characterization of such size shifting and its impact on

[2] The MSDS data of nanoclay, cloisite 20A, from manufacturer website, http://www.scprod.com/msds/Cloisite%2020A.pdf.

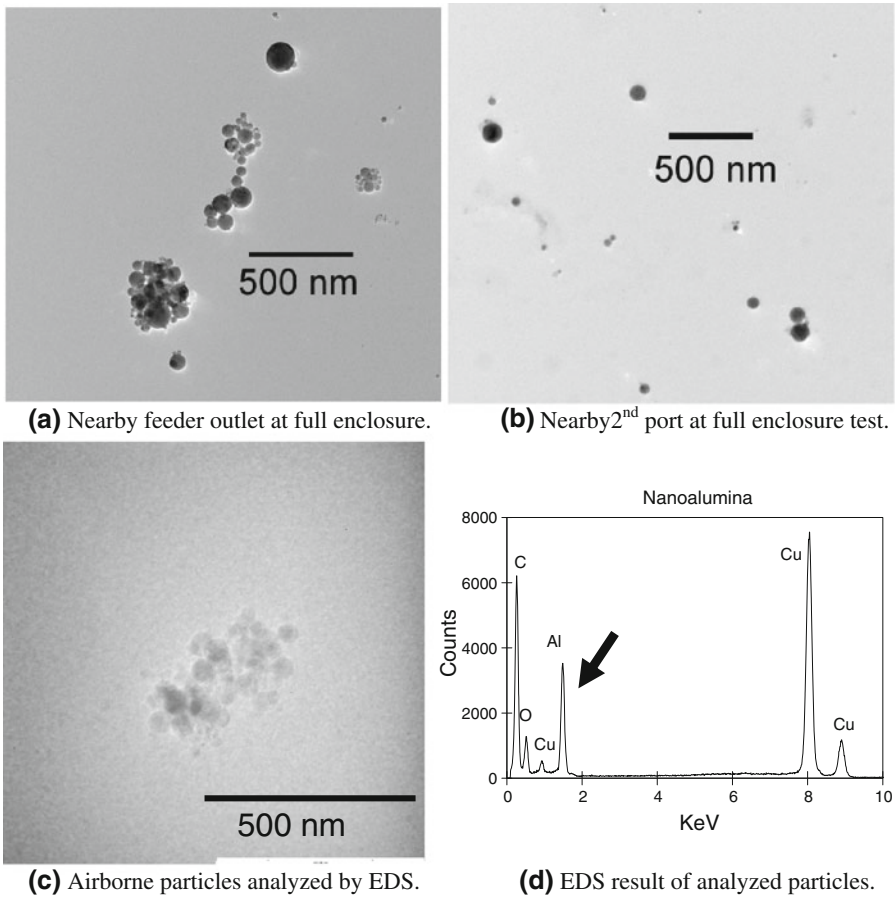

(a) Nearby feeder outlet at full enclosure. **(b)** Nearby2nd port at full enclosure test.

(c) Airborne particles analyzed by EDS. **(d)** EDS result of analyzed particles.

Fig. 6 TEM images of *nanoalumina* particles and EDS results

exposure assessment associated with the variety of particle morphology and agglomerates will need substantial effort and investment in research and technology.

Engineering control strategies

Feeding caused the greatest nanoparticle release when no isolation was applied to the throat due to the dispersing of continuously fed materials for the length of the experiment. Isolation applied to the feeding throat dramatically reduced the nanoparticle release, and the hopper enclosure successfully contained nanoparticles and prevented their escape during the loading procedure. Using both enclosures successfully reduced the particle concentration around releasing sources close to, or below, the pre-test baseline level.

The modified loading procedure was designed to have the hopper hold approximately one kilogram of nanoparticles to be dropped by gravity from the hopper two-step compartments to the feeder. The air movement inside the hopper induced by the falling granular material could cause suspended airborne nanoparticles to escape through small gaps in the hopper. Therefore, the vented acrylic enclosure was designed and placed over the hopper and the vented air flow between the hopper and the acrylic enclosure captured such escaping nanoparticles. In addition, the air flow through the slot openings created theoretically sufficient high-capture velocities in the immediate vicinity of the feeder itself. The capture velocity was estimated by Eq. 1 to be 100 m/min at a 15-cm radius from the slots, sufficient to capture any particles released in the immediate vicinity of the enclosure slots. However, the second feeding port, which released polymer fume mixed with deagglomerated nanoparticles, could not be directly enclosed due to the high-temperature surface, and the capture velocity at

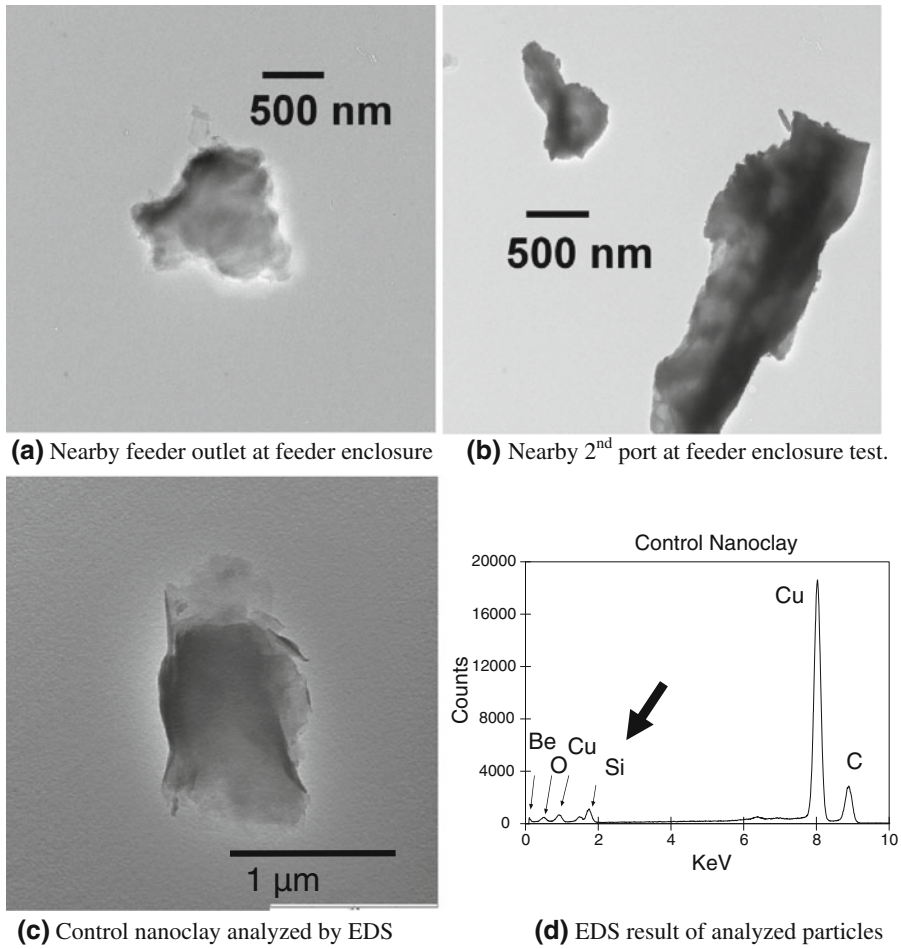

Fig. 7 TEM images of *nanoclay* particles and EDS results

(a) Nearby feeder outlet at feeder enclosure **(b)** Nearby 2nd port at feeder enclosure test.

(c) Control nanoclay analyzed by EDS **(d)** EDS result of analyzed particles

the second feeding port induced by the airflow entering the opening slots of the hopper enclosure was much reduced. This capture velocity was calculated using Eq. 1. In this case, the air flow was 11.3 m^3/min, the slot length was 0.20 m, and the distance from the slot to the 2nd port was 0.74 m. Substituting into Eq. 1, obtained the capture velocity of 20.6 m/min (67 ft/min).

$$V(x) = \frac{11.3\,\mathrm{m}^3/\,\mathrm{min}}{3.7(0.20\,\mathrm{m})(0.74\,\mathrm{m})} = 20.6\,\mathrm{m}/\,\mathrm{min}(67\ \mathrm{ft}/\mathrm{min})$$

This value of capture velocity is relatively low; according to the American Conference of Governmental Industrial Hygienists (ACGIH) (ACGIH 2007), it is appropriate for contaminants that are "released with practically no velocity into quiet air." Nanoparticles have essentially zero inertia and, thus, are always released with "no velocity," favoring low-capture velocities. However, turbulent air flow surrounding the 2nd port was obvious and caused by the hot venting air, heating equipment (>400 °C) and operator's hand motion and walking nearby. This characterizes the conditions around the second port in our laboratory and indicates that the air flow through the enclosure slots likely was not creating a sufficiently high-capture velocity to capture contaminants released from the 2nd port. That led to the escape of nanoparticles from the 2nd port, which then migrated in the low-velocity air stream toward the feeding throat as seen from collected airborne particles shown in Figs. 6 and 7. Capture and removal of such individual nanoparticles released from the 2nd port were crucial to reduce migration of those nanoparticles. However, engineering control could not be applied directly to the 2nd port due to process limitations including the lack of an available local exhaust ventilation duct, the high-temperature extruder surface, and heated air at the 2nd port.

Nanoparticles are small enough that gravity settling can be neglected and released nanoparticles would be suspended in the air and be carried with the invisible air stream. The workers' arm and body motion likely caused increased airflow turbulence in the vicinity of the extruder. Operator's standing area for loading material and checking control panel and the operator's moving area for checking mixing condition at 2nd port and extruded products are marked in Fig. 3. When the air flow created by the *full enclosure* exhaust system is effective in collecting particles from the near-field, in order to control the far-field, then the air velocities must be sufficient to overcome the random velocities created by the thermal updrafts and the turbulent air flow induced in the wake region due to workers' motion. Consequently, this requires a fairly high-air flow through the hopper vent. However, that may increase the loss of valuable nanomaterials/nanoparticles in production and significantly increase energy use, pointing to the need for developing optimal engineering control strategies for nanomaterial/nanoparticle production processes such as the one studied here. In addition, the captured nanoparticles will be transported through the duct and discharged to the atmosphere if air pollution control devices were absent or inadequate. The ability of standard air pollution control devices such as fabric filters and electrostatic precipitators to effectively remove nanoparticles has not been widely studied and requires significant further research.

Conclusion

The challenge of exposure assessment and control can be seen from results of this study. Exposure assessment requires measuring the quantity of aerosols released by the process into a time-varying BG concentration. With regard to controls, some sources such as the hopper and feeder can be effectively controlled with enclosure and ventilation, but other sources such as the 2nd port must rely on capturing released nanoparticles which is made more difficult by the complex airflow pattern in the room. In some situations, the quantity of particles released into the room did not exceed the variable baseline aerosol concentration, or the air flow and capture velocity were sufficient to quickly remove the small number of particles released and thus not cause a concentration increase, which could be mistakenly interpreted as no release for this situation. This study showed that the full enclosure reduced particle concentrations to below the baseline, but the instruments used could not detect possible trace amounts of nanoparticle release, and the operational environment used pilot-scale equipment and thus should be typically seen in industry and some laboratories. Collection and characterization of airborne particles were essential for exposure assessment in order to identify the presence of released nanoparticles of concern.

In summary, while isolation is regarded (after substitution or process change) as being the highest priority among engineering control methods (Burgess et al. 2004), it has to be properly designed and applied to each specific industrial process producing nanoparticles in order for sufficient nanoparticle containment to be attained. When the isolation cannot be applied, or results in insufficient containment, ventilation is the next priority of the control hierarchy. Depending on the particular application, ventilation may be used alone or in combination with isolation, as was done in this study. As shown here, ventilated enclosures can be extremely effective at controlling nanoparticle release. Whenever capture ventilation is used, however, the airflow pattern/path plays a very important role in determining the system's effectiveness in removing nanoparticles. Investigating the characteristics of the air flow surrounding the equipment is necessary for designing a proper local ventilation system; the use of flow visualization techniques such as fog release is frequently helpful in this regard since submicron particles and nanoparticles will have same moving path as released fog. In considering possible solutions from the perspective of cleaner production, improving the bonding force of fillers (nanoparticles) to polymer would reduce or eliminate free nanoparticles released during production and potentially during the life-cycle use of nanocomposite products. However, this would require substantial research into the interfacial bonding of nanomaterials/nanoparticles with the polymer matrix.

The controls designed and applied in this study sufficiently reduced exposure to operators. For the environmental and workers' secondary protection, air pollution control is also required to be applied to the vented exhaust to capture released nanoparticles. When studying exposure issues, identifying and understanding contributing factors such as ventilation

use, process isolation, and airflow patterns in the near- and far-fields as evaluated in this study are essential to performing a systematic exposure assessment and developing the optimal control strategies.

Schulte et al. (2010) concluded that performance-based engineering controls, control banding, and interim occupational exposure limits can be useful steps to minimize the health risks to workers and to serve as a means for assessing the effectiveness of exposure control measures and making other risk management decisions. For many practical workplaces and environments, the aforementioned factors vary considerably and require careful study. Managing and documenting such variables affecting exposure are essential for exposure assessment, since the combination of factors such as specific exhaust system design and air flow used in any particular application would otherwise mislead actual exposure results and/or cause inadequacy or confounders for epidemiological study and medical surveillance when the exposure data from various locations were aggregated. In order to successfully control airborne contaminants associated with nanoparticle use, integrating control strategies such as isolation and ventilation, as reported in this study, with filtration or other air pollution methods is essential to managing exposure and risk.

Acknowledgments Authors would like to acknowledge the financial support from the Nanoscale Science and Engineering Center for High-rate Nanomanufacturing (CHN) funded by the National Science Foundation (Award No. NSF-0425826), the Program of Research Education for Undergraduate students associated with CHN, and the collaboration with National ChiaoTung University funded by the Taiwan Institute of Occupational Safety and Health (Grant No. IOSH98-H324). Doctoral student ChunChia Huang and technician Christopher Santeufemio of UMASS Lowell provided support for the TEM image analysis.

Conflict of Interest The authors declare no conflict of interest.

References

ACGIH (2007) Industrial ventilation: a manual of recommended practice for design. American Conference of Governmental Industrial Hygienists, Cincinnati

Bottini M, Magrini A, Bottini N, Bergamaschi A (2003) Nanotubes and fullerenes: an overview of the possible environmental and biological impact of bio-nanotechnologies. Med Lav 94:497–505

Burgess WA, Ellenbecker MJ, Treitman RD (2004) Ventilation for control of the work environment. Wiley-Interscience, New York

Ferin J, Oberdorster G, Penny DP, Soderholm SC, Gelein R, Piper HC (1990) Increased pulmonary toxicity of ultrafine particles? I. Particle clearance, translocation, morphology. J Aerosol Sci 21:381–384

Ferin J, Oberdörster G, Soderholm S, Gelein R (1991) Pulmonary tissue access of ultrafine particles. J Aerosol Med 4:57–68

ICRP (1994) International Commission on Radiological Protection Publication 66: human respiratory tract model for radiological protection. Elsevier, Oxford

Kim TH, Flynn MR (1991a) Airflow pattern around a worker in a uniform freestream. Am Ind Hyg Assoc J 52:287–296

Kim TH, Flynn MR (1991b) Modeling a worker's exposure from a hand-held source in a uniform freestream. Am Ind Hyg Assoc J 52:458–463

Maynard AD, Kuempel ED (2005) Airborne nanostructured particles and occupational health. J Nanopart Res 7(6):587–614. doi:10.1007/s11051-005-6770-9

McCarrie KM, Winter R (2003) Properties of epoxy-clay nanocomposite adhesives for bonded strap joints. San Jose State Report

Oberdorster G, Ferin J, Finkelstein J, Wade P, Corson N (1990) Increased pulmonary toxicity of ultrafine particles? II. Lung lavage studies. J Aerosol Sci 21:387

Popendorf W (2006) Industrial hygiene control of airborne chemical hazards. Taylor & Francis, Boca Raton

Renwick LC, Brown D, Clouter A, Donaldson K (2004) Increased inflammation and altered macrophage chemotatic responses caused by two ultrafine particle types. Occup Environ Med 61:442–447

Schulte PA, Murashov V, Zumwalde R, Kuempel ED, Geraci CL (2010) Occupational exposure limits for nanomaterials: state of the art. J Nanopart Res 12:1971–1987

Takenaka S, Dornhofer-Takenaka H, Muhle H (1986) Alveolar distribution of fly ash and of titanium dioxide after long-term inhalation by Wistar rats. J Aerosol Sci 17:361–364

Tsai SJ, Ashter A, Ada E, Mead J, Barry C, Ellenbecker MJ (2008a) Airborne nanoparticle release associated with the compounding of nanocomposites using nanoalumina as fillers. Aerosol and Air Qual Res 8:160–177

Tsai SJ, Ashter A, Ada E, Mead J, Barry C, Ellenbecker MJ (2008b) Control of airborne nanoparticle release during compounding of polymer nanocomposites. NANO 3:1–9

Tsai SJ, Ada E, Isaacs J, Ellenbecker MJ (2009) Airborne nanoparticle exposures associated with the manual handling of nanoalumina in fume hoods. J Nanopart Res 11:147–161. doi:10.1007/s11051-008-9459-z

Wolff RK, Henderson RF, Eidson AF, Pickrell JA, Rothenberg SJ, Hahn FF (1988) Toxicity of gallium oxide particles following a 4-week inhalation exposure. J Appl Toxicol 8:191–199

Zhang Q, Kusaka Y, Donaldson K (2000) Comparative pulmonary responses caused by exposure to standard cobalt and ultrafine cobalt. J Occup Health 42:179–184